LIMNOLOGY
and
OCEANOGRAPHY

ASLO

Limnol. Oceanogr. 9999, 2020, 1–17

doi: 10.1002/lno.11684

Why productive lakes are larger mercury sedimentary sinks than oligotrophic brown water lakes

Martin Schütze ,[1*] **Philipp Gatz**,[1] **Benjamin-Silas Gilfedder** ,[2] **Harald Biester** [1]

[1]Institut für Geoökologie, AG Umweltgeochemie, Technische Universität Braunschweig, Braunschweig, Germany
[2]Lehrstuhl für Hydrologie, Universität Bayreuth, Bayreuth, Germany

Abstract

Mercury accumulation in lake sediments is a widespread environmental problem due to the biomagnification of Hg in the aquatic food chain. Soil Hg concentrations, catchment vegetation, erosion, and lake productivity are major factors controlling the accumulation of Hg in lakes. However, their influence on the Hg mass balance in lakes with different catchment characteristics and trophic state is poorly understood. In this multilake study, we decipher the effects of catchment vegetation (coniferous vs. deciduous forest), soil Hg content, and trophic state on Hg sedimentation at six lakes in Germany. We investigated Hg concentrations in leaves, soils, and the lake's water phase. Soils under coniferous stands show slightly higher Hg concentrations than under deciduous forest. Hg concentrations in the water phase were higher in the oligotrophic brown water lakes (8.1 ± 5.6 ng L^{-1} vs. 3.0 ± 1.9 ng L^{-1}). Lower Hg concentrations in sediment trap material indicate dilution by algae organic matter in the mesotrophic lakes (0.12–0.17 μg g^{-1} vs. 0.57–0.89 μg g^{-1}). However, Hg accumulation rates in sediment traps were up to 14-fold higher in the mesotrophic lakes (113–443 μg m^{-2} yr^{-1}) than in the brown water lakes (32–144 μg m^{-2} yr^{-1}), which could not be explained by higher Hg fluxes to the productive lakes. Hg mass balance calculation reveals that water phase Hg scavenging by algae is the major reason for the intense Hg export to the sediments of productive lakes which makes them significantly larger sedimentary sinks than oligotrophic brown water lakes.

Mercury is a toxic pollutant of global concern that is known for its biomagnification in aquatic food chains. Due to the enrichment of methyl-Hg (MeHg) in fish, understanding the biogeochemical cycling of Hg in lakes is crucial. Lakes integrate catchment characteristics and processes and are often a major sink of pollutant (Moser et al. 2019). Thus, most Hg in lakes is received from the atmosphere via direct atmospheric deposition. Subsequent processes as leaching and erosion of catchment soils, or transport via streams and rivers are widely accepted to be the main transport pathways for Hg found in limnic systems. Atmospheric Hg enters forest ecosystems via wet and dry deposition (Hintelmann et al. 2002; St. Louis et al. 2019). Approximately 65–90% of this input is through stomatal uptake of elemental Hg (Hg^0) (Demers et al. 2007; Jiskra et al. 2015; Enrico et al. 2016). Hence, litterfall accounts for most of the Hg flux to forest soils, although the extent of this process, as well as transport to downstream waters, may differ between coniferous and deciduous forests (Woerndle et al. 2018). Higher Hg concentrations have been observed in the litter of coniferous than those in deciduous forests (Schwesig and Matzner 2000; Obrist et al. 2012), and the highest Hg accumulation is in the organic horizons of coniferous forest soils (Gruba et al. 2019). Moreover, needles of evergreen coniferous trees provide a larger surface area for Hg uptake when regarding the leaf/needle surface area on an annual basis (i.e., no leaf surface area in deciduous forests in winter) (Obrist et al. 2012; Navrátil et al. 2014). This difference may result in higher Hg concentrations in coniferous litter than in litter from deciduous forests, which in turn may result in a higher Hg flux to the forest floor in coniferous forest stands (Grigal et al. 2000; Johnson et al. 2007). However, others have demonstrated that Hg concentrations in coniferous litter are lower than those in deciduous litter (Sheehan et al. 2006; Demers et al. 2007; Navrátil et al. 2016). In a recent study, Wohlgemuth et al. (2020) demonstrated higher foliar Hg uptake per leaf area in broad leaves than in current-season conifer needles.

Drenner et al. (2013) found a significant linear relationship between Hg levels in largemouth bass (*Micropterus salmoides*)

*Correspondence: martin.schuetze@tu-bs.de [Technische Universität Braunschweig]

Additional Supporting Information may be found in the online version of this article.

and the percentage of landscape covered by coniferous forest but not with percent land coverage by deciduous forest. Particulate organic matter (POM) and dissolved organic matter (DOM) are major transport vectors of Hg from forests to lakes owing to the enrichment of Hg present in the organic soil horizons (Klaminder et al. 2008; Biester et al. 2012; Jiang et al. 2018). Similarly, a higher percentage of peatlands in the catchment is related to both higher DOM and higher Hg concentrations in lake water (Laudon et al. 2004; Wiener et al. 2006). Previous studies on Holocene palynological and geochemical data derived from lake sediments indicate a significant increase in Hg concentrations when catchment vegetation shifted from deciduous to coniferous vegetation during the Holocene (Rydberg et al. 2015; Schütze et al. 2018).

In a lake's water phase, Hg is predominately associated with DOM, POM, as well as minerogenic particles and settles to the lake bottom along with the sediments (Gascón Díez et al. 2016). Algae and algal-derived organic matter (OM) have been shown to take up or scavenge Hg from the water column (Mason et al. 1995; Dranguet et al. 2014). The scavenging of Hg by algae has been shown to have a major influence on Hg cycling in lakes (e.g., speciation), being a major vector for Hg accumulation in aquatic sediments (Biester et al. 2018; Zaferani et al. 2018), and a key driver for promoting Hg accumulation in lake sediments since industrialization (Outridge et al. 2007; Faucheur et al. 2014). Some studies have found no relationship between algal productivity and Hg accumulation in sediments (Kirk et al. 2011; Cooke et al. 2012), while others have suggested that terrestrial inputs may obscure the signal from algal scavenging (Sanei et al. 2012; Brazeau et al. 2013). Studies based on Hg mass balance calculations argue that algal blooms may dilute Hg concentrations in algal-derived OM (Pickhardt et al. 2002; Karimi et al. 2007). The idea that Hg scavenging or uptake by algae affects Hg accumulation in lake sediments is widely accepted. However, the extent of Hg scavenging by algae, how this relates to trophic state, and its role in the accumulation of Hg in lake sediments has not yet been investigated. Moreover, the OM source appears to be crucial for the production of MeHg in lake sediments and the lake's water phase. Bravo et al. (2017) showed that phytoplankton-derived organic compounds increase Hg methylation rates (k_m = 0.038–0.075 d^{-1}) in boreal lake sediments through an overall increase in bacterial activity and low concentrations of MeHg (1.3—2.8 ng g^{-1}), while lake sediments dominated by terrigenous OM inputs display significantly lower methylation rates (k_m = 0.0095–0.013 d^{-1}) but relatively high concentrations of MeHg (3.7—8.0 ng g^{-1}). In addition, MeHg is known to be formed in forest soils and is transported to lakes by POM and DOM (Tsz-Ki Tsui et al. 2019), although the role of different forest vegetation in lake catchments on water phase Hg concentrations and Hg accumulation in lake sediments is poorly understood.

In the present study, we investigated six lakes in two mountain areas in Germany, which differ in catchment vegetation (coniferous vs. deciduous forest) and in-lake primary productivity. To decipher the effect of these parameters on Hg concentrations and accumulation in the lake sediments, we investigated catchment soils, inflow, and lake water Hg concentrations, along with Hg sedimentation rates in sediment traps over a period of 2 yr. In addition, we used C/N ratios and Fourier-transform infrared spectroscopy (FTIR) to determine the dominant sources of OM in the different lake systems.

Materials and methods

Study areas

The two study areas are located in the eastern Harz Mountains (HZ) and the northern Black Forest (BF) in Germany (Fig. 1A) and are defined as low mountain ranges, a typical geographical feature of Central Europe. In contrast to high-altitude mountains such as the High Alps, the summits at the studied mountain sites do not reach the tree line, which results in seasonal litterfall in the catchments of the forest lakes.

In the Harz Mountains, we investigated three small reservoirs: Großer Siebersteinteich (GT), Kleiner Siebersteinteich (KT), and Großer Dachsteich (DT). These mesotrophic to eutrophic reservoirs were constructed during the 18th century for fisheries. Nowadays, the lakes are predominantly used for flood control and local recreation, as these waterbodies are located near the provincial town of Ballenstedt (Fig. 1B) where settlements are partly downstream of the lake outflows. The catchment soils are dominated by base-rich brown earth and brown earth podzols from rubble loess over loamy graywacke debris (BGR Geoviewer 2018). The steep flanks of the reservoirs are covered in deciduous stands with oak (*Quercus robur*), beech (*Fagus sylvatica*), maple (*Acer platanoides*), and birch (*Betula pendula*). Smaller areas with mountain pines (*Pinus mugo*) are found in the north-west flank of Lake GT.

In the Black Forest, we investigated three small headwater cirque oligotrophic brown water lakes: Herrenwiesersee (HS), Schurmsee (SS), and Glaswaldsee (GS). The anthropogenic pressure on the lakes is relatively low as there are no settlements in the catchments (Fig. 1C). The catchment topography was formed in a cirque excavated by glaciers, so the cupped sections of the three lakes are relatively steep. Acid podzols and Triassic sandstone rubble dominate the catchments at those sites (BGR Geoviewer 2018). The catchments are densely covered by coniferous forests dominated by spruce (*Picea abies*). An overview of the geographical characteristics of the investigated lakes and their catchments is shown in Table 1. Meteorological data on annual precipitation, frost days, solar radiation, and sunshine duration are shown for both studied areas in the Supporting Information Fig. S1. The graphical representation of all catchment areas is shown in Supporting Information Figs. S2–S7.

Sampling and sample treatment

Litter and soil samples

We collected forest litter and soil samples (n = 69), including a few tree leaves/needles, from five lake catchments (GS,

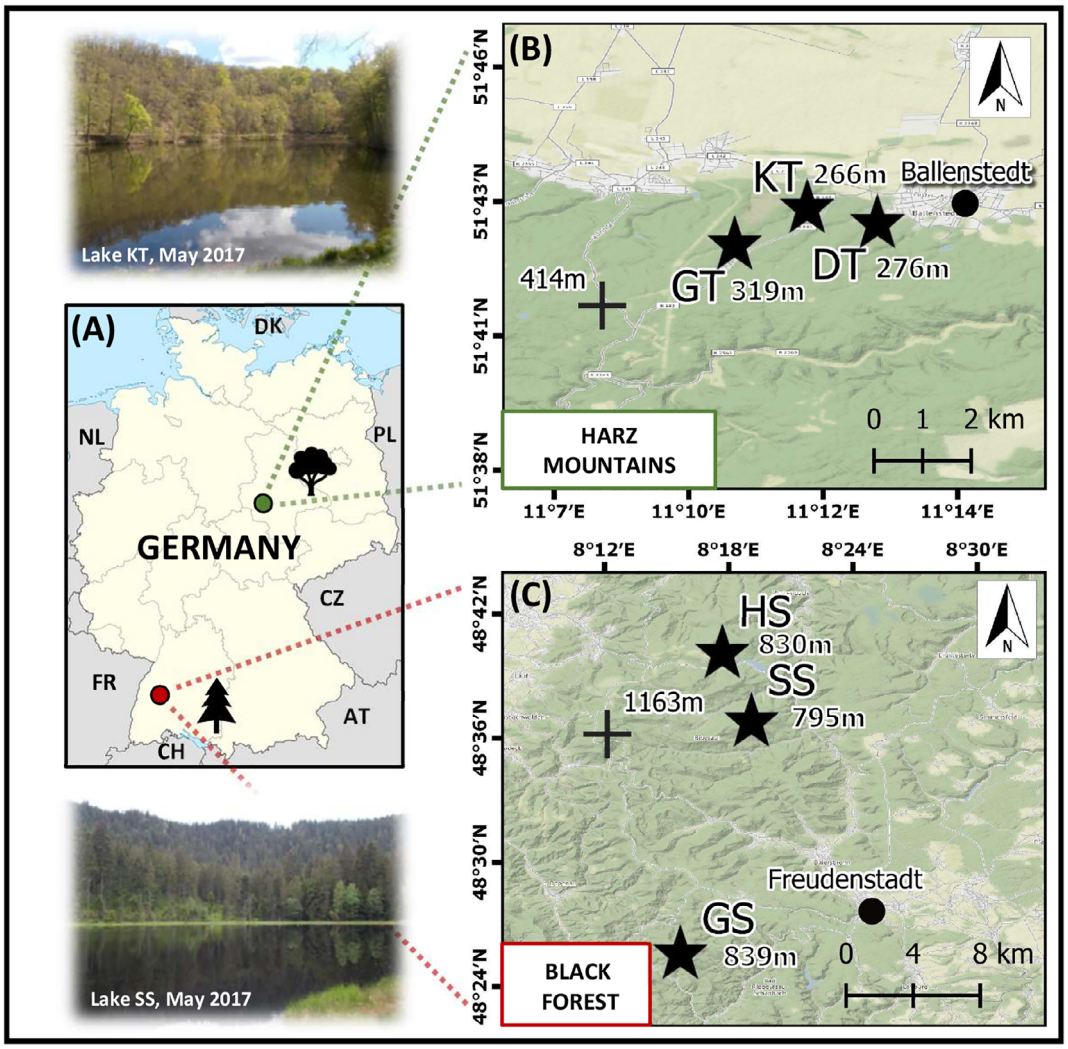

Fig. 1. (**A**) Location of the two sampling areas in Germany. (**B**) Eastern Harz Mountains. (**C**) Northern Black Forest. The studied lakes are indicated with black stars, mountain summits with black crosses.

SS, GT, KT, and DT) from at least three randomly chosen plots per stand in April 2017. For more details, see the Supporting Information (Interactive map file: sampling locations.kmz). Soil samples were taken using a Pürckhauer-corer and five subsamples were combined from each sampling plot (1 × 1 m). Samples encompassed fresh and dry leaves/needles, two litter horizons (Oi: undecomposed surface litter; Oa: fully decomposed humus layer) and one mineral soil layer at a depth of 15–20 cm. These four individual sample compartments are described below as foliage, litter, organic, and mineral soil. Sampling of solid samples was conducted using Nitril gloves and cleaned stainless steel equipment. All samples were packed into plastic bags (Whirl-Pak, U.S.A.), stored at 4°C during the fieldwork and at −20°C in the laboratory until they were freeze-dried, and ground using an agate ball mill (Retsch, Germany).

Lake water phase

In total, 226 water samples were collected from the GS, SS, GT, KT, and DT lakes between June 2016 and November 2017. Samples were taken at 1 m depth intervals from the surface to the maximum water depth using a 1.5-liter water sampler (Uwitec, Austria). In addition, water samples from the direct inflows and outflows of the lakes were taken if permitted by hydrologic conditions. Electrical conductivity (EC), pH, and oxygen concentrations were determined in the field using portable meters (Cond 3110, pH 3110, and Multi 3510 IDS, WTW GmbH, Germany). All samples were filtered in the field using nylon membrane filters (0.45 μm, Carl Roth GmbH, Germany) after preconditioning the filters using a small amount of sample and stored in disposable polypropylene tubes (50 mL, Sarstedt, Germany) at 4°C until analysis. Subsamples for dissolved organic carbon (DOC) and cation determination were not stabilized and measured within 2–3 d after sampling. Subsamples for major and trace element analyses were stabilized by adding 1% (v/v) of bi-distilled nitric acid (HNO_3, Merck AG, Germany). Subsamples for Hg analyses were stabilized following USEPA–Method 1631 using 1% (v/v) ultrapure BrCl–HCl solution (Merck AG).

Table 1. Geographical characteristics by area and its dominant forest type, lake designation, code, location, altitude, lake depth, surface area, catchment area, and their ratios of all investigated lakes.

Area	Forest type	Lake	Code	Location	Altitude (m a.s.l.)	Lake depth (m)	Surface area (km^2)	Catchment area (km^2)	Surface/ catchment
BF	Coniferous forest	Herrenwiesersee	HS	48°40′6.84″N 8°17′43.90″E	830	10	0.018	0.369	1:21
		Schurmsee	SS	48°36′47.61″N 8°19′7.86″E	795	13	0.015	0.506	1:34
		Glaswaldsee	GS	48°25′32.53″N 8°15′44.40″E	839	11	0.030	0.592	1:20
HZ	Deciduous forest	Großer Siebersteinteich	GT	51°42′30.84″N 11°10′31.98″E	319	12	0.034	2.950	1:88
		Kleiner Siebersteinteich	KT	51°43′8.26″N 11°11′43.84″E	266	5	0.017	1.200	1:70
		Großer Dachsteich	DT	51°42′49.28″N 11°12′58.34″E	276	5	0.026	1.360	1:52

Sediment traps

Sediment traps (n = 13) were deployed in all six lakes. The traps consisted of two acrylic glass tubes (single tube surface area of 55.4 cm^2), two connected sediment containers (2 L, Polypropylene, Nalgene, U.S.A.), a weight anchor, and buoys. At each location, the top edge of the sediment trap was placed approximately 1.5 m above the sediment surface. The sediment traps were installed in the lake water column during spring and autumn (122–208 d) (Supporting Information Fig. S9C). To evaluate the seasonal influence on the sedimentation rate and/or the trap material composition, the sediment traps GS2017 and GS2018 in the Harz Mountains were also installed during the winter period, for 335 d and 487 d, respectively. The sedimentary residues, including the overlying water column, were stored at −20°C. The entire trap content was freeze-dried and ground in an agate mortar. Subsamples of sediment trap material were digested using bi-distilled nitric acid (HNO_3, Merck AG) for 1 h at 180°C (CEM Mars 5 Microwave system, U.S.A.).

Sediment cores

To investigate the temporal variations in element concentrations, four short lake sediment cores (13–29 cm) were taken from the lake centers using a gravity corer (Uwitec, Austria). After sampling, cores were kept upright and stored at 4°C, sliced at a resolution of 1 cm (HS) or 2 cm (SS, GS, GT) using acid-washed plastic tools. Samples (n = 64) were packed into plastic bags (Whirl-Pak, U.S.A.), stored at −20°C, freeze-dried, and ground using an agate ball mill (Retsch, Germany).

Laboratory and data analyses

Solid samples

The Hg content in the solid samples was analyzed by thermal decomposition followed by preconcentration of Hg on a gold trap and cold vapor atomic absorption spectrophotometry using a DMA-80 direct mercury analyzer (Milestone, Italy). The total concentrations of Al as an indicator of mineral matter fluxes from the catchment to the lake sediment cores were analyzed using energy-dispersive X-ray fluorescence (Cheburkin and Shotyk 1996). The major and trace element concentrations in the digests from sediment trap material were determined either by ICP-OES (Varian 715-ES, Agilent, U.S.A.) (Mg, K, Ca, Fe, and Cu) or by ICP-MS (Agilent 7700, U.S.A.) (Al, Zr, V, and Cr). The total carbon and nitrogen concentrations in the solid samples were determined using a Euro EA 3000 elemental analyzer (HEKAtech GmbH, Germany). The samples of trap material from five of the investigated lakes (GS, SS, GT, KT, and GT) were analyzed by FTIR using a Vector 22 FTIR spectrometer (Bruker, Germany) in absorption mode, with subsequent baseline subtraction on KBr pellets (200 mg dried KBr and 2 mg sample). Measurements were recorded from 4.500 to 600 cm^{-1}. Sample imaging of the trap material was conducted using a Phenom XL desktop (Thermo Fischer Scientific, U.S.A.) scanning electron microscope (SEM). The SEM conditions utilized for imaging were a 15 kV accelerating voltage, approximately 8 mm working distance, ×5000 magnification, and a backscattering electron detector.

Water samples

Total Hg concentrations in the water samples were measured by means of cold vapor atomic fluorescence spectrometry (mercur, Analytik Jena AG, Germany) after removing excess BrCl by adding hydroxylammonium chloride (0.5% v/v) and stannous chloride Hg^{2+} reduction.

Major and trace element concentrations were determined either by ICP-OES (Varian 715-ES, Agilent, U.S.A.) (Mg, Ca, Fe, and Cu) or by ICP-MS (Agilent 7700, U.S.A.) (Al, Zr, V, and Cr). Filtered water samples were analyzed for total DOC using

thermo-catalytic oxidation at 950°C with subsequent non-dispersive infrared (NDIR) detection of CO_2 using a TOC analyzer (multi N/C 2100, Analytik Jena AG, Germany). Concentrations of nitrate and chloride were analyzed by ion chromatography with chemical suppression and conductivity detection (761 Compact IC, Metrohm, Switzerland).

Analytical quality assurance

For each analytical technique, blanks and sample replicates were determined. Standard reference materials (SRMs) were analyzed to assure analytical quality. The following SRMs were used: trace metals in surface water SPS-SW1 and RTC 1-WP, river water NRC SLRS-5, Thames LGC6019, MAURI-09, and ORMS-5, soil NCS DC 73322, sediment CANMET-LKSD-4, IAES-SL-1, and NCS DC 73312, apple leaves NIST 1515, pine needles NIST 1575a, and poplar leaves GBW07604. For more details, see the Supporting Information Table S5.

Modeled atmospheric deposition

To compare atmospheric Hg fluxes in the two study areas, we estimated the local Hg atmospheric deposition (Hg_{AT}) to the forest soils using an ecosystem-specific modeled data set for 2016 and 2017 (MSC-E 2018). The atmospheric deposition rate of Hg was provided by MSC-E of EMEP (Co-operative Programme for Monitoring and Evaluation of Long-range Transmission of Air Pollutants in Europe). Deposition fluxes of Hg across Germany are based on the chemical transport model "MSCE_HM" (Travnikov and Ilyin 2005). For this study, the data set "evergreen needleleaf forests" was chosen for the locations in the Black Forest. Owing to the presence of mountain pines at the northwest flank of Lake GT, the data set "mixed forest" was used to estimate Hg deposition rates in the deciduous forest-dominated Harz Mountains.

Results

Hg soil concentrations

The results of soil Hg analyses for all studied sites show that mean Hg concentrations were highest in the organic-rich and lowest in the mineral horizon. The mean Hg concentration in litter was generally lower than in the organic-rich, but higher than that in the mineral horizon. Mean concentrations of Hg in the organic horizon in the Black Forest ($0.284 \pm 0.128\ \mu g\ g^{-1}$) were slightly higher than those in the Harz Mountains ($0.227 \pm 0.099\ \mu g\ g^{-1}$). On the other hand, the mineral horizon had lower mean concentrations of Hg in BF soils ($0.045 \pm 0.017\ \mu g\ g^{-1}$) than in HZ soils ($0.090 \pm 0.041\ \mu g\ g^{-1}$). The Hg concentration in litter at the BF sites ($0.140 \pm 0.026\ \mu g\ g^{-1}$) was similar to that at the HZ sites ($0.141 \pm 0.042\ \mu g\ g^{-1}$). However, the variability of Hg concentrations in the litter from deciduous forest stands was higher (29.8% vs. 18.8% RSD) than in the coniferous stands. In this study, we investigated a few leaves taken directly from the trees. The concentration of Hg in withered beech ($0.075\ \mu g\ g^{-1}$) and oak ($0.067\ \mu g\ g^{-1}$) leaves sampled in the Harz Mountains in November 2017 was higher than that in 1-yr-old green spruce needles ($0.038\ \mu g\ g^{-1}$ at GS and $0.053\ \mu g\ g^{-1}$ at SS). In contrast, the Hg concentration in the shoots of beech leaves sampled in March 2017 was significantly lower ($0.003\ \mu g\ g^{-1}$) than that in any other sample, indicating Hg enrichment by up to a factor of ~ 25 during the vegetation period.

The type of vegetation affects soil formation and cycling of OM and trace elements in terrestrial ecosystems (Smolander et al. 2005; Hansson et al. 2011; Wang et al. 2019). Thus, we determined the relationship between Hg concentrations and the chemical composition (C and N) of the soil samples (Fig. 2). The Hg ($\mu g\ g^{-1}$) to C ($g\ g^{-1}$) mass ratio indicates the degree of saturation of the soil OM with Hg. In both study areas, Hg/C ratios increased with depth (Supporting Information Fig. S8). In the Black Forest, average Hg/C ratios in organic ($0.92 \pm 0.09\ \mu g\ g^{-1}$) and mineral ($1.28 \pm 0.38\ \mu g\ g^{-1}$) soil horizons are similar to values reported from comparable forest soils in Poland and the Czech Republic (Navrátil et al. 2016; Gruba et al. 2019). In contrast, the average Hg/C ratios in organic ($3.10 \pm 1.12\ \mu g\ g^{-1}$) and mineral

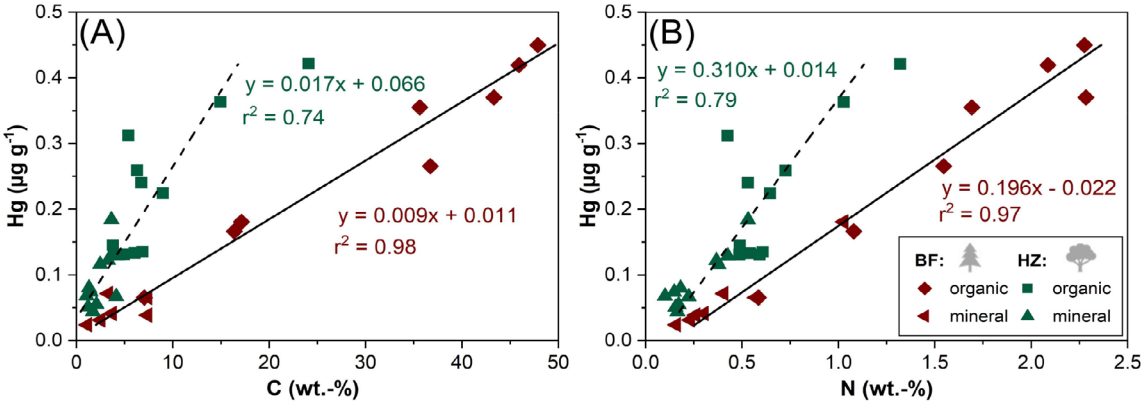

Fig. 2. Concentration of Hg in organic and mineral soil samples of deciduous (HZ) and coniferous (BF) forest stands as a function of carbon (**A**) and nitrogen (**B**). Coefficient of determination (r^2) denoted by the trend lines were at a significance level of $p < 0.05$.

($4.11 \pm 1.46\ \mu g\ g^{-1}$) soil horizons were higher than those in the Harz Mountains and exhibited greater variability between sampling points. The degradation rates, as indicated by the C/N ratios, of near surface OM exhibited high variance (Supporting Information Fig. S8A) and differ by tree species (Demers et al. 2007; Obrist et al. 2011). Figure 2 shows the correlation of Hg to C and N, respectively, for the organic and mineral soil horizons. Hg concentrations were positively correlated with the concentrations of C and N in both studied areas. However, soil samples from the coniferous BF showed consistently stronger correlations with Hg concentrations than soil samples from the HZ.

Chemical characteristic of the lake water phase

Figure 3 shows water depth profiles for pH, temperature, nitrate (NO_3^-), DOC, Hg, and Al of one lake representative for each study area (May and November 2017). The concentrations of dissolved Hg were more than twofold higher and showed higher variance in the BF lakes ($8.1 \pm 5.6\ ng\ L^{-1}$) than in the HZ lakes ($3.0 \pm 1.9\ ng\ L^{-1}$). Similarly, concentrations of DOC were about twice as high in the BF lakes ($13.8 \pm 5.4\ mg\ L^{-1}$) than in the HZ lakes ($6.8 \pm 1.9\ mg\ L^{-1}$).

The DOC values in the BF lakes decreased toward the lake's surface, which was not observed in the HZ lakes. Mean pH values of the lake water profiles as well as of the in- and outflows show that pH is lower at the BF sites (4.5 ± 0.3) compared to the HZ sites (7.7 ± 0.5). The high pH values in the upper 5 m of the HZ lakes (up to pH 9) clearly indicate high photosynthesis activity in the HZ lakes, which seems to be low in the BF lakes. EC was lower at the BF sites ($23.1 \pm 8.5\ \mu S\ cm^{-1}$) compared to the HZ sites ($373 \pm 96\ \mu S\ cm^{-1}$) (Supporting Information Table S4). Even greater differences were observed at the two study areas for Al (BF: $557 \pm 135\ \mu g\ L^{-1}$ and HZ: $14.3 \pm 8.8\ \mu g\ L^{-1}$). At the coniferous sites, Pearson correlation coefficients (r) for Hg to DOC ($r = 0.82$) and Al ($r = 0.80$) as well as DOC to Al ($r = 0.77$) were significant and positive, while r values for the same elements showed lower positive correlations (i.e., $r < 0.50$) or even no significant relationship to Hg or DOC in the HZ lakes (Supporting Information Table S4). The water depth profiles of Hg and Al corresponded to the DOC concentration at Lake SS (panel A) and demonstrate an enrichment of these elements in the water layer above the sediment, which could not be observed in the HZ lakes. Furthermore, the Hg, DOC, and Al showed higher concentrations in the inflow and outflow in November compared to May, while only minor differences in concentration between the two sampling dates were observed in the HZ lakes. NO_3^- concentrations were generally higher in the BF lakes and did not show a pronounced decline in the photic zone as observed in the HZ lakes, where NO_3^- concentrations were inversely related to pH, both indicating the generally higher phytoplankton productivity in the HZ lakes. Nitrate was the highest in the inflow of the HZ lakes, up to $3\ mg\ L^{-1}$, while it tended to be less than $1.5\ mg\ L^{-1}$ in the BF lakes.

Chemical composition of trap material

The trap material obtained from the two sampling areas showed large differences in quantity (Supporting Information Fig. S9C), texture, and color (Supporting Information Fig. S10A), biological residues derived from pollen, spores, and diatoms (Fig. 4A) as well as in their chemical composition. To better visualize these differences, the relative elemental composition is shown in relation to the simplified total amount (100%) of several major (Mg, K, Al, Fe, N, and C) elements. The non-normalized element concentrations of major and trace elements obtained in the sediment traps are given in Supporting Information Table S1. The normalized distribution of major elements indicated that OM is the major component in the traps from both sites. Normalized major elements (Fig. 4B) in the trap material from the BF lakes showed higher proportions of organic carbon (87%) compared to those found in the lakes from the Harz Mountains (62%). The mean relative proportions of nitrogen were similar at both sites (5–8%), whereas iron (14%), aluminum (12%), magnesium (3%), and potassium (3%) were a factor of 9, 4, 4, and 2, respectively, higher in the traps of the HZ lakes, indicating higher fluxes of soil-derived mineral matter to these lakes.

Trace elements (Supporting Information Fig. S10B) showed site-specific variation in the Black Forest, while element proportions, especially for copper, chromium, vanadium, and calcium, only slightly varied at the Harz Mountains. The highest concentrations (Supporting Information Table S1) of chromium ($65\ mg\ kg^{-1}$) and vanadium ($87\ mg\ kg^{-1}$) were found in the trap material of Lake KT. Both metals may have been emitted from a nearby country road (Supporting Information Fig. S3), which is consistent with the higher concentration of chlorine in the water phase, which may be attributed to the use of road salt during winter (Supporting Information Table S4). However, notable concentrations of copper were also observed in a sediment trap of the Black Forest, which is consistent with the geochemical signals found in the lake sediment of medieval mining activities near the lake catchments (Schütze et al. 2018).

Hg concentrations and accumulation rates in sediment traps

Sediment traps in the BF lakes showed low and relatively constant annual mass accumulation rates compared to the HZ lakes, where mass accumulation rates were up to a factor of 57 higher and varied from 1 yr to the next (Supporting Information Fig. S9C). Similarly, mean Hg accumulation rates in the BF lakes ($32–144\ \mu g\ m^{-2}\ yr^{-1}$) were up to a factor of 14 lower than in the HZ lakes ($113–443\ \mu g\ m^{-2}\ yr^{-1}$) (Fig. 5C). In contrast, the mean Hg concentrations (Fig. 5B) in trap material derived from the coniferous sites ($0.57–0.89\ \mu g\ g^{-1}$) were up to a factor of 7.4 higher than at the deciduous sites

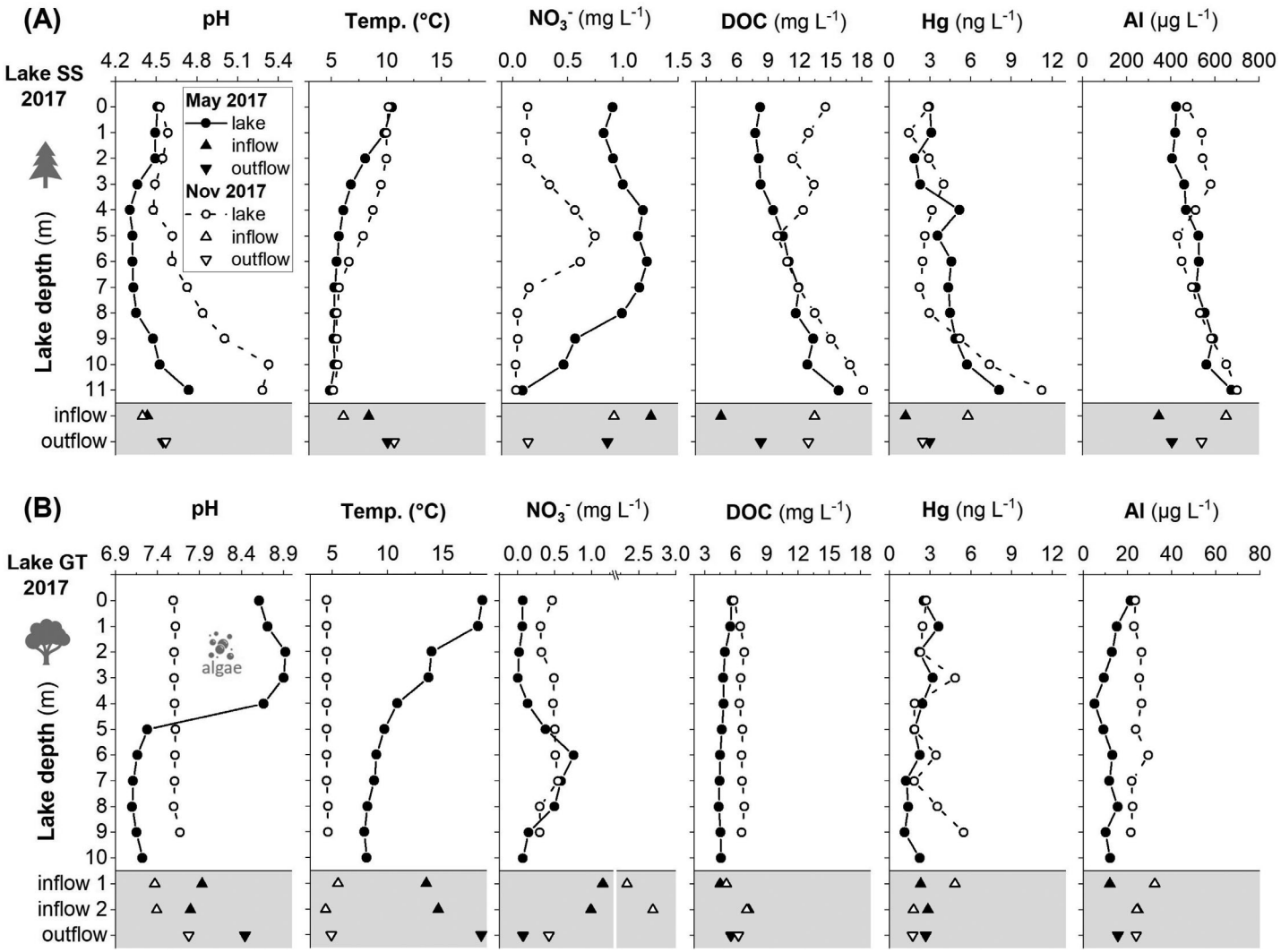

Fig. 3. Chemical characteristics (pH, temperature, NO_3^-, DOC, Hg, and Al) of lake water, and in- and outflows of two sampling campaigns at two selected representative lakes: Lake SS (**A**) and Lake GT (**B**) in May 2017 (black symbols) and November 2017 (open symbols). Notice the different scaling for pH, NO_3^-, and Al concentrations at SS and GT.

(0.12–0.17 $\mu g\ g^{-1}$). The highest sediment trap Hg concentration was observed at Lake GS in the Black Forest during the summer of 2018, when the mean sunshine duration was high, and the mean precipitation was low (Supporting Information Fig. S9A,B). In comparison, the highest Hg accumulation rate was observed at Lake KT in the Harz Mountains in 2016, a year with an unusually warm springtime in Germany.

To understand the interdependencies between the catchment and in-lake processes, it is essential to differentiate between OM sources. Terrestrial plants have a higher C/N ratio (~ 25) than aquatic algae (< 10) (Meyers and Ishiwatari 1993), although decomposed soil OM can have significantly lower C/N ratios than plant material. The mean C/N ratios of the trap material from the BF lakes (13.9 ± 3.0) pointed to a terrestrial dominated OM source, while the low C/N ratios in the trap of the HZ lakes (8.5 ± 0.6) indicate algae as the main source of OM in all three lakes (Fig. 5A). However, it has to be pointed out here, that the C/N-ratios in the catchment soils of the HZ lakes also had values below 10; thus, the C/N-ratios alone do not prove that algae is the main OM source. However, the high pH (> 8) in May (Fig. 3B) and the distribution of nitrate concentrations in the water column relative to the inflow clearly indicated the high phytoplankton productivity in these lakes. Moreover, the FTIR spectra (Fig. 6) also supported a higher influence of algae in the HZ lakes compared to the BF lakes.

Spectral information of trap material

The FTIR spectra analyses were performed using the Peak Analyzer Peak Fit Gaussian function (OriginPro 2018). The spectral information showed that the trap material from the lakes in both study areas was received from both

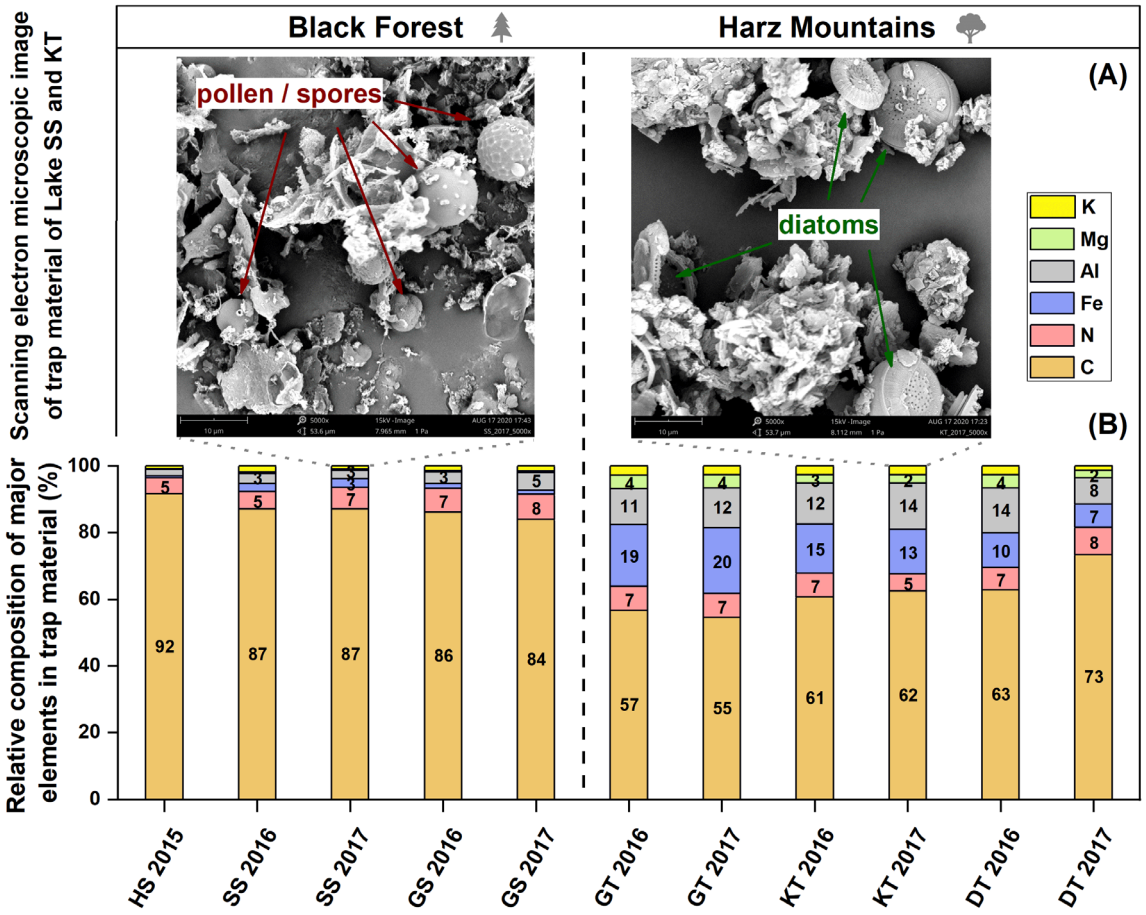

Fig. 4. Examples of scanning electron microscopic images (**A**) of freeze-dried trap material of Lake SS and KT (2017) showing residues of pollen, spores, and diatoms with a ×5000 magnification. Relative composition of major elements in trap material (**B**) received from BF and HZ lakes. Values of the stacked bars give the percentage in relation to the total amount (100%) of the selected major elements.

autochthonous and allochthonous sources (i.e., mixture of algal, microbial, and land plant detritus). This assumption was supported by absorptions peaks associated with polysaccharides (1080 cm^{-1}), humic and fulvic acids (1410 cm^{-1}), secondary amines (1640 cm^{-1}), and aliphatic compounds (2850 and 2920 cm^{-1}), which could be observed in all six lakes (Fig. 6 and Supporting Information Table S3). Polysaccharides were highly abundant in the HZ lakes, while the BF lake trap material was dominated by secondary amines and humic and fulvic acids. A weak peak associated with lignin (1210 and 1266 cm^{-1}) occurred solely in the trap material of the BF lakes (HS, GS, and SS). The spectra of the trap material of the HZ lakes (GT, KT, and DT) had peaks associated with (biogenic-) silica (690 and 780 cm^{-1}) and a small peak indicating proteins (1543 cm^{-1}), typical for microalgae (Dean and Sigee 2006), which was not observed in the BF lakes.

Sediment geochemistry derived from short cores

In the BF lakes (Fig. 7A–C), sediment Hg concentrations generally decreased with depth and peaked at the sediment surface layer with 1.55 $\mu g\ g^{-1}$ at HS, 0.68 $\mu g\ g^{-1}$ at SS, and 0.90 $\mu g\ g^{-1}$ at GS. In contrast, the short core of the mesotrophic Lake GT in the Harz Mountains (Fig. 7D) shows the highest Hg concentration (0.25 $\mu g\ g^{-1}$) at a depth of 14 cm, with lower concentrations in the surface layer (0.12 $\mu g\ g^{-1}$).

The C/N ratios in all sediment cores show relatively constant values indicating that OM sources did not drastically change over time. The three sediment cores from the BF lakes had C/N ratios that varied between 10.9 and 16.1, with a mean value of 13.3, whereas the C/N ratios in the single HZ core were clearly lower (8.3 ± 0.33) than in the BF cores, as found in the sediment traps. Al concentrations were relatively constant in all sediment cores, indicating that strong erosion events were rare. Similar to those observed in the sediment traps, Al concentrations in the BF sediments (1.9 ± 1.2 wt.%) were approximately 50% lower than in the HZ lake sediment (2.9 ± 0.4 wt.%), indicating higher fluxes of lithogenic material at Lake GT.

Discussion

Factors influencing the distributions of Hg in the soil horizons

Concentrations of Hg in forest soils are highly dependent on tree species. In coniferous forests, the Hg content in OM-

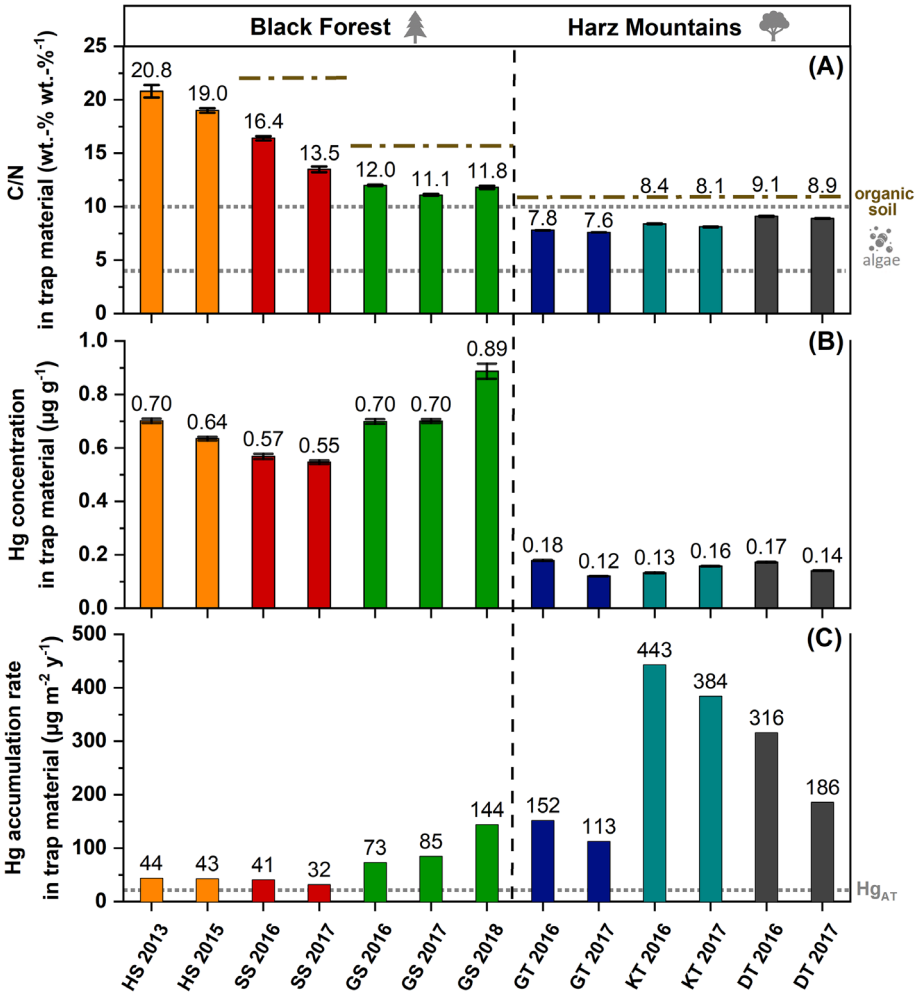

Fig. 5. Comparison of the composition of trap material installed during several years in all investigated lakes. Panel (**A**) shows the C/N ratio, marked with values of organic soil and a range typical for OM derived from algae (Meyers and Ishiwatari 1993). Differences in Hg concentration (**B**) and Hg accumulation rate (**C**), marked with a mean Hg atmospheric deposition value (Hg_{AT}, ecosystem-specific EMEP-model for the year 2016) for both studied areas in panel (**C**).

rich horizons is often higher than in deciduous forests (Schwesig and Matzner 2000; Obrist et al. 2012; Navrátil et al. 2016). The results of this study confirm these findings, although the Hg concentrations in the organic-rich soil horizons of the BF soils were only slightly higher than those of the deciduous forests in the HZ. In addition to the uptake by leaves and the extent of litterfall, Hg concentrations in the soils of both sites might be additionally influenced by local climatic factors, such as annual precipitation, rainfall intensity, days with frost, solar radiation, sunshine duration, and wind speed (Hararuk et al. 2012; Rydberg and Martinez-Cortizas 2014; Siudek et al. 2016; Baptista-Salazar and Biester 2019). The number of frost days, solar radiation, and sunshine duration were comparable in both study areas (Supporting Information Fig. S1), whereas the annual precipitation rate is more than threefold higher in the Black Forest (1344 mm) than at the Harz Mountains (406 mm).

Based on the ecosystem-specific modeled data set, the estimated atmospheric Hg deposition rates at the BF study sites were 50% higher ($\sim 27\ \mu g\ m^{-2}\ yr^{-1}$) than those at the Harz sites ($\sim 18\ \mu g\ m^{-2}\ yr^{-1}$). The ecosystem-specific deposition rates for both study areas were comparable to those reported for other forest sites in the Czech Republic and the northern U.S.A. ($9–34\ \mu g\ m^{-2}\ yr^{-1}$) (Blackwell and Driscoll 2015; Navrátil et al. 2016; St. Louis et al. 2019). Blackwell and Driscoll (2015) showed that atmospheric Hg deposition increases with elevation and the dominant deposition pathway shifts from litterfall in low-elevation hardwoods to throughfall in mid-elevation spruce and fir dominated forests. Throughfall in coniferous forests has been shown to increase Hg deposition in soils (Sheehan et al. 2006; Witt et al. 2009; Gerson et al. 2017). Furthermore, the needles of conifers have a higher surface area and roughness (i.e., leaf structure) which reduces air circulation and increases particle adsorption

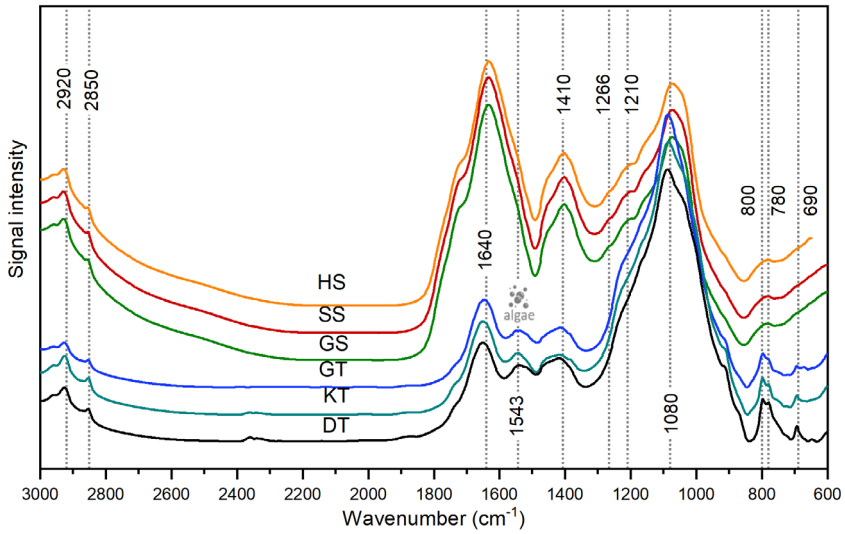

Fig. 6. FTIR spectra of sediment trap material sampled in lakes in the Black Forest (HS, GS, and SS) and in the Harz Mountains (GT, KT, and DT). Extract of wavenumber intensities 600–3000 cm^{-1} (staggered for better visualization). Bands typical for the trap material are highlighted accordingly.

(Demers et al. 2007; Johnson et al. 2007). This promotes the adsorption and accumulation of Hg on needles and may result in increased Hg concentrations in the needles and the soil of coniferous forests. Based on these findings, the higher throughfall in coniferous BF stands (Demers et al. 2007; Witt et al. 2009) is likely the dominant Hg deposition pathway to

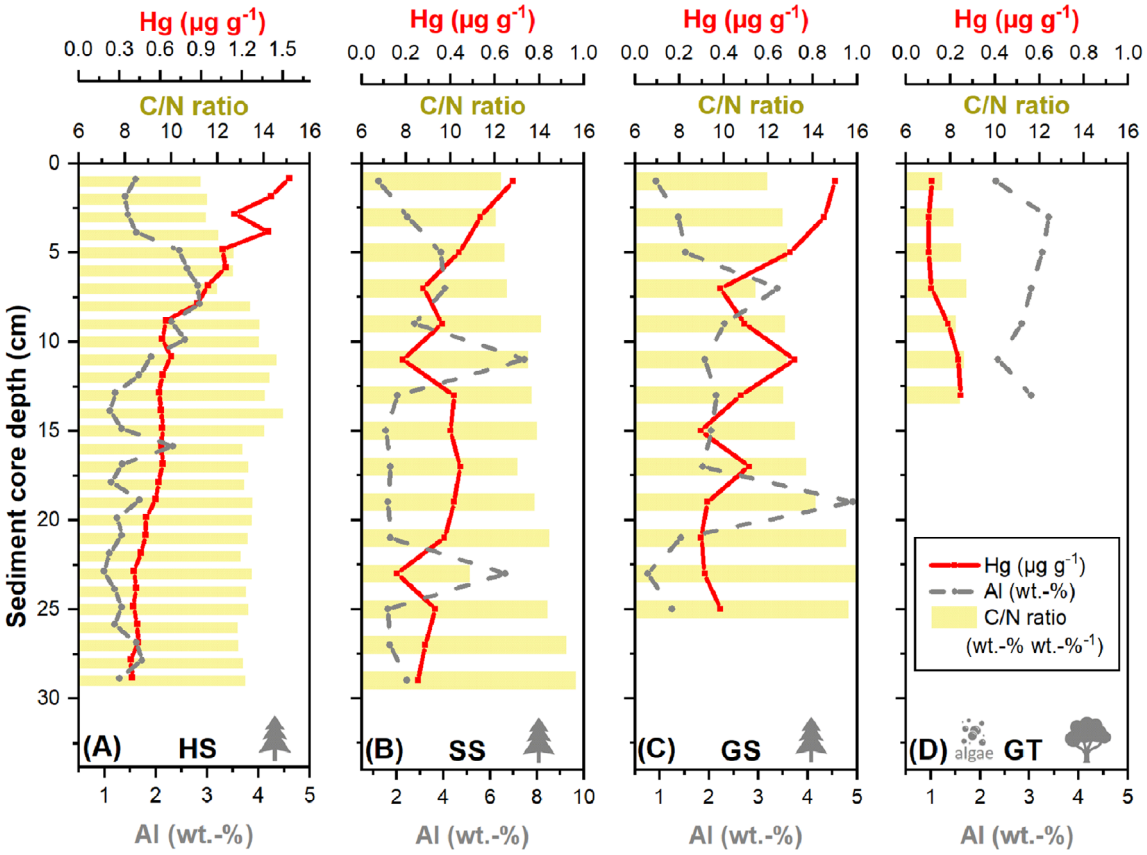

Fig. 7. Down-core profiles of the lake sediments of HS, SS, GS (Black Forest, **A**–**C**) and GT (Harz Mountains, **D**) present carbon/nitrogen ratios (yellow bars) as an indicator for organic matter sources, concentrations of Hg (red line), and concentrations of Al (gray dashed line) as an indicator of mineral matter erosion from the lake catchments.

the soils at the BF sites. Moreover, the mean altitude at the BF sites was ~ 530 m higher (Table 1) than at the HZ sites, which might further support higher atmospheric deposition in the BF. In contrast, deciduous forests are thought to show higher net Hg accumulation in litter than coniferous forests due to differences in litter dynamics (Demers et al. 2007; Navrátil et al. 2016; Wohlgemuth et al. 2020). On the other hand, the generally higher litter mass in deciduous forests leads to a dilution of Hg concentrations (Obrist et al. 2012), which would explain the slightly lower Hg levels in the organic soil of the deciduous forest sites in the HZ.

Coniferous forests produce acidic soils that facilitate higher humic acid-rich DOC production compared to deciduous forests (Navrátil et al. 2016). This is confirmed by the higher DOC concentrations in the BF lakes and their in- and outflows (Fig. 3), which was also reported in a catchment study of Lake HS (Steinhoefel et al. 2017). Due to the high binding affinity of Hg to DOM (Biester et al. 2004; Rydberg et al. 2010; Teisserenc et al. 2011), the higher DOC concentration in the BF lakes explain the high Hg concentration in, and also suggests higher Hg fluxes to the BF lakes as suggested in previous studies (Rydberg et al. 2015).

Effect of soil erosion on sediment Hg concentrations and accumulation rates

Although the mean Hg concentrations in the organic soil horizon in coniferous forests of the BF were only slightly higher than those in the deciduous forests of the HZ, Hg concentrations in the trap material and the sediments differed significantly between the two sites. Hg concentrations in the surface sediment layer of Lake GS are more than twofold higher than the highest Hg concentration found in the BF catchment soils. In the HZ, surface sediments of Lake GT show only half the maximum Hg concentration found in the catchment soils, which indicates a dilution process in the Harz lakes. The catchments of the six lakes are considerably larger than the lake surface area (Table 1); thus, sediment Hg accumulation rates depend, to a large extent, on Hg fluxes from the catchment soils (Rydberg et al. 2015). The amount of Hg transported from catchment soils to lakes is regulated by the flux of mineral particles relative to DOM and POM fluxes, where Hg concentrations in DOM and POM are usually higher than in mineral matter (Hermanns and Biester 2013). Previous studies have demonstrated a strong relationship between Hg concentrations in the sediment and DOM mobilization in catchment soils (Kolka et al. 1999; Ouellet et al. 2009). Dilution of organic bound Hg by mineral matter has been shown in several lake sediment studies (Thevenon et al. 2011; Hermanns and Biester 2013; Pompeani et al. 2018) and is also apparent in the sediment cores from our study sites (Fig. 7), where an inverse correlation between Hg and Al (mineral matter) concentrations has been observed. The different chemical compositions of trap material from the two sites clearly indicate that Hg concentrations in the HZ trap sediments were diluted by mineral matter and likely by autochthonous OM resulting from high phytoplankton productivity. In contrast, Hg accumulation rates in the HZ sediment traps were up to a factor of 14 higher than in the BF sediment traps, which cannot be explained by higher Hg fluxes from the catchments. Our results indicate that algae OM appear to dilute Hg concentrations in trap materials but also greatly enhance Hg accumulation rates. High Hg accumulation in sediments as a result of Hg scavenging by algal OM in the water column has been described in previous studies (Outridge et al. 2007, 2019; Zhang et al. 2014; Biester et al. 2018; Zaferani et al. 2018), although the source and mass balance of Hg in these studies was mostly unknown.

Hg concentrations in the HZ sediment traps (Fig. 5B) were within the range of total Hg concentrations found in the sediment traps (0.08–0.26 $\mu g\ g^{-1}$) of Lake Geneva found by Gascón Díez et al. (2016). They concluded that Hg and OM in the settling particles originated primarily from phytoplankton. Gascón Díez et al. (2016) observed also that Hg concentrations strongly decreased in the sediment traps of Lake Geneva during spring and remained low until autumn, when primary productivity decreased, indicating a dilution of Hg concentrations in traps by algal-derived OM similar to what has been observed in the Harz traps (Figs. 5B, 7 and Supporting Information Fig. S10B). In contrast, the chemical composition of the small headwater BF cirque lakes indicated dominant terrestrial Hg sources, predominately DOM-Hg fluxes, and revealed annual differences in Hg concentration in the trap material caused by changes in hydrological conditions. Furthermore, higher OM fluxes from the surrounding catchment resulted in higher Hg to C ratios (Supporting Information Table S1) in the BF sediment traps because terrigenous OM is generally older and more degraded than autochthonous OM (Ouellet et al. 2009; Jiskra et al. 2015).

Outridge et al. (2019) argued in a recent study that inconsistent findings in sediment Hg concentrations vs. the extent of primary productivity relationship in some northern lakes and shallow ponds might be due to differences in lake and catchment properties which limit the amount of Hg that is available for scavenging in the water column by algae. Accordingly, at similar atmospheric Hg deposition rates and comparable soil Hg content, a larger catchment area would result in higher Hg accumulation rates in the lake sediments. Thus, the higher amount of mineral matter found in the traps of the HZ lakes may imply that higher Hg accumulation rates are attributed to higher erosion or larger catchments to lake ratios of these sites.

Figure 8 illustrates the relationship between Hg accumulation in sediment traps and catchment area. Although there were only few lakes, the results indicate a moderate positive catchment area effect for the BF lakes and a negative relationship for the HZ lakes. Lake KT, which had the highest Hg accumulation rate, had a 2.5-fold smaller catchment area than Lake GT, indicating that catchment area does not explain the

high Hg accumulation rates in the HZ lakes. Moreover, precipitation rates in the BF study area were significantly higher than in the HZ, which facilitates high erosional fluxes in the BF lakes.

Role of aquatic productivity on Hg accumulation

Our results showed that differences in atmospheric Hg deposition fluxes, catchment area, or erosional fluxes cannot explain the high Hg accumulation rates in the HZ lakes. Similar to what has been observed in other lakes (Biester et al. 2018; Outridge et al. 2019) or the ocean (Zaferani et al. 2018), we suggest that water column Hg scavenging by sinking algal OM strongly increases Hg export from the water phase to the sediment in the HZ lakes. The chemical composition of the trap material of the HZ lakes (low C/N ratios, polypeptides, amides, and proteins indicated by the FTIR spectra) as well as in the water phase (high pH, low nitrate) gives a clear indication that OM in the HZ lake sediments is dominated by algal-derived OM in contrast to the BF lakes, where most OM is derived from catchment soils (Fig. 3B, Supporting Information Table S4). Furthermore, SEM images indicated a high abundance of diatom frustules in the trap material of the HZ, while diatoms were found only rarely in BF traps.

To evaluate the effect of water phase Hg scavenging, we calculated the annual number of Hg water column depletions ($n \times Hg_{dpl}$) necessary to balance the Hg flux to the sediment (Eq. 1). We neglected the Hg flux to the lakes by the inflow as well as Hg re-emission from the lake surfaces, which were not determined in this study. Here, we assume that the water column Hg inventory is derived from Hg transported to the lake by leaching/erosion as DOM/POM-Hg from the catchment and via direct atmospheric Hg deposition. Hg contributes to maintaining a steady Hg inventory in the lake. The Hg inventory (Hg_{pwc}) was calculated using the mean Hg concentration in the water phase times the volume of the water column (m^3) above the trap.

$$n\,Hg_{dpl} = \frac{Hg_{trap}}{Hg_{pwc}} \quad (1)$$

Equation 1 is a simplified equation for calculating the number of Hg water column depletion events (Hg_{dpl}) necessary to obtain the Hg mass balance in the investigated lakes. Hg_{trap} and Hg_{pwc} are in $\mu g\ m^{-2}\ yr^{-1}$.

Thus, Lake GS had a mean Hg concentration in the water column (Hg $conc_{w.column}$) of 11 ng L^{-1} (2017), which amounts to 105 μg Hg in the water column above 1 m^2 of the lake bed and a water column ($V_{w.column}$) of 9.5 m above the sediment trap. This corresponds to an Hg water inventory of 105 $\mu g\ m^{-2}\ yr^{-1}$. Using Eq. 1 results in n Hg_{dpl} = 0.8, which explains the annual Hg flux of 85 $\mu g\ m^{-2}\ yr^{-1}$ to the sediments (Fig. 5C). The calculation of n Hg_{dpl} for the other BF lakes even show values below 0.8. Thus, a single Hg scavenging event in the lake water column could explain the entire annual Hg accumulation rate in the BF sediment traps. Due to this ancillary role of water phase Hg scavenging and the fact that the water phase Hg pool in the BF lakes is likely to be continuously refilled by inflow, atmospheric Hg deposition or erosion, and surface run-off, we conclude that the Hg mass balance in the BF lakes is mainly controlled by catchment fluxes, atmospheric deposition, and Hg export through outflows or Hg re-emission to the atmosphere and to a minor extent by export to the sediments.

In contrast, n Hg_{dpl} for the HZ lakes ranges between 4 and 55 (Table 2), indicating the large importance of the water phase Hg scavenging needed to build up the high Hg accumulation rates in the HZ lake sediments. Moreover, scavenging is not a process restricted to Hg. Al and trace elements were highly depleted in the water phase (Fig. 3) but accumulated in the sediment traps (Fig. 4 and Supporting Information Fig. S10) of the productive Harz Mountains lakes compared to the brown water lakes in the Black Forest.

The discrepancy in rates of sedimentation and Hg accumulation between Lake GT (113–152 $\mu g\ m^{-2}\ yr^{-1}$) with a catchment area of ~ 3 km^2 and Lake KT (384–443 $\mu g\ m^{-2}\ yr^{-1}$) with a catchment area of ~ 1.2 km^2 (Fig. 8) emphasizes the role of phytoplankton productivity for Hg accumulation in these lakes. The HZ lakes showed no significant differences in chemical composition or Hg concentrations in the water phase, but Lake GT is twice as deep as Lake KT (Fig. 5B and Supporting Information Fig. S10B, Table S1). Kerimoglu and Rinke (2013) demonstrated that cyanobacteria blooms occurred in a

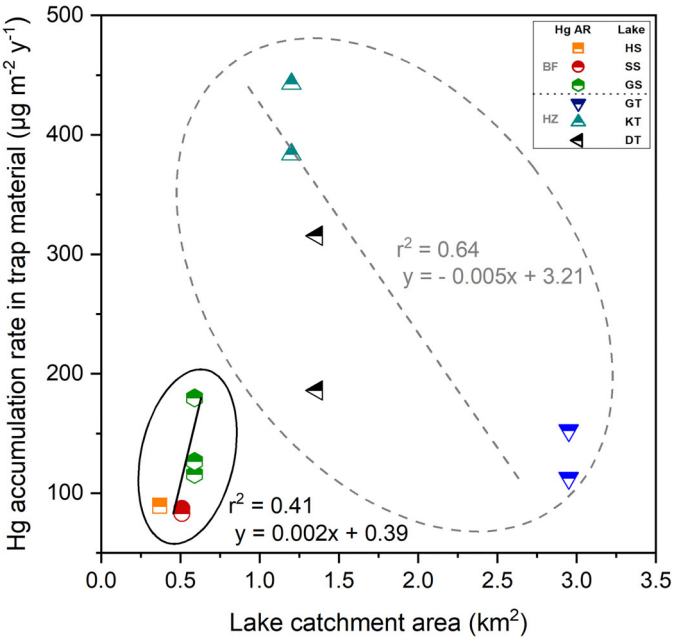

Fig. 8. Relationships between Hg accumulation rates in sediment trap material and lake catchment area for the lakes in study areas BF and HZ. Regression equations and *r* values for these variables are shown.

Table 2. Individual values of a simplified calculation to calculate the number of Hg water column depletion events (n Hg_{dpl}) required to balance the Hg flux to the sediment in the investigated lakes.

Area	Trap	Hg_{AT} ($\mu g\ m^{-2}\ yr^{-1}$)	Hg_{trap} ($\mu g\ m^{-2}\ yr^{-1}$)	Hg $conc_{w.column}$ ($ng\ L^{-1}$)	$V_{w.column}$* (L)	Hg_{pwc} ($\mu g\ m^{-2}\ yr^{-1}$)	n Hg_{dpl} (n)
BF	SS 2016	27	41	4.3	11,500	49	0.8
	SS 2017	27	32	4.0	11,500	46	0.7
	GS 2016	26	73	12.5	9500	119	0.6
	GS 2017	26	85	11.0	9500	105	0.8
HZ	GT 2016	18	152	2.8	10,500	29	5.2
	GT 2017	18	113	2.7	10,500	28	4.0
	KT 2016	18	443	2.3	3500	8	55
	KT 2017	18	384	2.2	3500	8	48
	DT 2016	17	316	4.2	3500	15	21
	DT 2017	17	186	4.1	3500	14	13

*Above the sediment trap inlet.

reservoir, particularly during years with low water levels enriched with nutrients. High production of autochthonous OM in shallow lakes resulted in anaerobic conditions and slow OM mineralization in the water phase, resulting in high sedimentation rates and intense scavenging of trace elements. In contrast to the BF lakes, the environmental fate of Hg in the HZ lakes is characterized by a strong export of Hg from the water phase to the sediment and a relatively low Hg export through the outflow. Thus, the HZ lakes with high primary productivity appear to be large Hg sedimentary sinks, whereas the BF brown water lakes show much lower Hg accumulation in the sediments and higher (DOM-) Hg throughflow. Our results support the findings of a model approach on the changes in Hg cycling in the Baltic Sea attributed to algae bloom events (Soerensen et al. 2016). These authors found that eutrophication enhances Hg export to the sediment and reduces Hg re-emission to the atmosphere (Figure 9).

Conclusions

We compared Hg accumulation in oligotrophic brown water lakes and mesotrophic to eutrophic lakes and catchment soils at two forested areas in Germany which differ in catchment vegetation (coniferous vs. deciduous forest) and weather conditions. Hg concentrations in soils were comparable at both sites but were clearly higher in the sediments of the brown water lakes. However, Hg accumulation rates derived from sediment traps of the productive lakes, where algae blooms are common, were increased by a factor of 14 higher than those derived from brown water lakes. Our data suggest that Hg scavenging and sedimentation by algal OM is

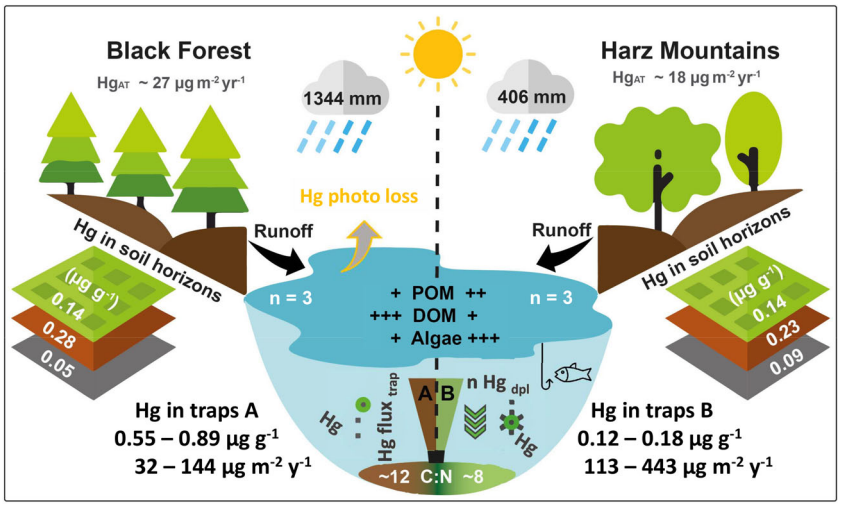

Fig. 9. Conceptual transport pathways of Hg from the soil horizons to the lake's water phase and lake sediments investigated in lake catchments of the Black Forest and the Harz Mountains, respectively.

primarily responsible for the high Hg accumulation rates found in the sediments of the productive lakes. Up to 55 times the water column Hg inventory was required to explain the fluxes in deciduous catchments while less than one depletion was needed for the brown water lakes. From this, we concluded that productive lakes are major sinks for catchment-derived Hg in contrast to brown water lakes, where throughflow and re-emission to the atmosphere are major export pathways for Hg and Hg accumulation in the sediments is less important. This further suggests that increasing eutrophication of aquatic systems as a result of high nutrient fluxes and increasing temperatures will turn more lakes into sedimentary Hg sinks. Due to the high OM content in the sediments and the resulting anaerobic condition, productive lakes are hot spots for methyl-Hg production and transfer to the aquatic food chain, which is subject to future increases.

References

Baptista-Salazar, C., and H. Biester. 2019. The role of hydrological conditions for riverine Hg species transport in the Idrija mining area. Environ. Pollut. **247**: 716–724. doi:10.1016/j.envpol.2019.01.109

BGR Geoviewer. 2018. German Federal Institute for Geosciences and Natural Resources [WWW document]. [accessed 2018 June 3]. Available from https://geoviewer.bgr.de

Biester, H., F. Keppler, A. Putschew, and M. Petri. 2004. Halogen retention, organohalogens, and the role of organic matter decomposition on halogen enrichment in two chilean peat bogs. Environ. Sci. Technol. **38**: 1984–1991. doi:10.1021/es0348492

Biester, H., Y. M. Hermanns, and A. Martínez Cortizas. 2012. The influence of organic matter decay on the distribution of major and trace elements in ombrotrophic mires - a case study from the Harz Mountains. Geochim. Cosmochim. Acta **84**: 126–136. doi:10.1016/j.gca.2012.01.003

Biester, H., M. Pérez-Rodríguez, B.-S. Gilfedder, A. M. Cortizas, and Y.-M. Hermanns. 2018. Solar irradiance and primary productivity controlled mercury accumulation in sediments of a remote lake in the Southern Hemisphere during the past 4000 years. Limnol. Oceanogr. **63**: 540–549. doi:10.1002/lno.10647

Blackwell, B. D., and C. T. Driscoll. 2015. Deposition of mercury in forests along a montane elevation gradient. Environ. Sci. Technol. **49**: 5363–5370. doi:10.1021/es505928w

Bravo, A. G., S. Bouchet, J. Tolu, E. Björn, A. Mateos-Rivera, and S. Bertilsson. 2017. Molecular composition of organic matter controls methylmercury formation in boreal lakes. Nat. Commun. **8**: 14255. doi:10.1038/ncomms14255

Brazeau, M. L., A. J. Poulain, A. M. Paterson, W. Keller, H. Sanei, and J. M. Blais. 2013. Recent changes in mercury deposition and primary productivity inferred from sediments of lakes from the Hudson Bay Lowlands, Ontario, Canada. Environ. Pollut. **173**: 52–60. doi:10.1016/j.envpol.2012.09.017

Cheburkin, A. K., and W. Shotyk. 1996. An energy-dispersive miniprobe multielement analyzer (EMMA) for direct analysis of Pb and other trace elements in peats. Fresenius J. Anal. Chem. **354**: 688–691. doi:10.1007/s0021663540688

Cooke, C. A., A. P. Wolfe, N. Michelutti, P. H. Balcom, and J. P. Briner. 2012. A holocene perspective on algal mercury scavenging to sediments of an Arctic lake. Environ. Sci. Technol. **46**: 7135–7141. doi:10.1021/es3003124

Dean, A. P., and D. C. Sigee. 2006. Molecular heterogeneity in *Aphanizomenon flos-aquae* and *Anabaena flos-aquae* (Cyanophyta): A synchrotron-based Fourier-transform infrared study of lake micropopulations. Eur. J. Phycol. **41**: 201–212. doi:10.1080/09670260600645907

Demers, J. D., C. T. Driscoll, T. J. Fahey, and J. B. Yavitt. 2007. Mercury cycling in litter and soil in different forest types in the Adirondack region, New York, USA. Ecol. Appl. **17**: 1341–1351. doi:10.1890/06-1697.1

Dranguet, P., R. Flück, N. Regier, C. Cosio, S. Le Faucheur, and V. I. Slaveykova. 2014. Towards mechanistic understanding of mercury availability and toxicity to aquatic primary producers. Chimia **68**: 799–805. doi:10.2533/chimia.2014.799

Drenner, R. W., M. M. Chumchal, C. M. Jones, C. M. B. Lehmann, D. A. Gay, and D. I. Donato. 2013. Effects of mercury deposition and coniferous forests on the mercury contamination of fish in the south central United States. Environ. Sci. Technol. **47**: 1274–1279. doi:10.1021/es303734n

Enrico, M., G. L. Roux, N. Marusczak, L.-E. Heimbürger, A. Claustres, X. Fu, R. Sun, and J. E. Sonke. 2016. Atmospheric mercury transfer to peat bogs dominated by gaseous elemental mercury dry deposition. Environ. Sci. Technol. **50**: 2405–2412. doi:10.1021/acs.est.5b06058

Faucheur, S. L., P. G. C. Campbell, C. Fortin, and V. I. Slaveykova. 2014. Interactions between mercury and phytoplankton: Speciation, bioavailability, and internal handling. Environ. Toxicol. Chem. **33**: 1211–1224. doi:10.1002/etc.2424

Gascón Díez, E., J.-L. Loizeau, C. Cosio, S. Bouchet, T. Adatte, D. Amouroux, and A. G. Bravo. 2016. Role of settling particles on mercury methylation in the oxic water column of freshwater systems. Environ. Sci. Technol. **50**: 11672–11679. doi:10.1021/acs.est.6b03260

Gerson, J. R., C. T. Driscoll, J. D. Demers, A. K. Sauer, B. D. Blackwell, M. R. Montesdeoca, J. B. Shanley, and D. S. Ross. 2017. Deposition of mercury in forests across a montane elevation gradient: Elevational and seasonal patterns in methylmercury inputs and production. J. Geophys. Res. Biogeosci. **122**:1922–1939. doi:10.1002/2016JG003721

Grigal, D. F., R. K. Kolka, J. A. Fleck, and E. A. Nater. 2000. Mercury budget of an upland-peatland watershed. Biogeochemistry **50**: 95–109. doi:10.1023/A:1006322705566

Gruba, P., J. Socha, M. Pietrzykowski, and D. Pasichnyk. 2019. Tree species affects the concentration of total mercury (Hg) in forest soils: Evidence from a forest soil inventory in Poland. Sci. Total Environ. **647**: 141–148. doi:10.1016/j.scitotenv.2018.07.452

Hansson, K., B. A. Olsson, M. Olsson, U. Johansson, and D. B. Kleja. 2011. Differences in soil properties in adjacent stands of Scots pine, Norway spruce and silver birch in SW Sweden. For. Ecol. Manage. **262**: 522–530. doi:10.1016/j.foreco.2011.04.021

Hararuk, O., D. Obrist, and Y. Luo. 2012. Modeling the sensitivity of soil mercury storage to climate-induced changes in soil carbon pools. Biogeosci. Discuss. **9**: 11403–11441. doi:10.5194/bgd-9-11403-2012

Hermanns, Y. M., and H. Biester. 2013. Anthropogenic mercury signals in lake sediments from southernmost Patagonia, Chile. Sci. Total Environ. **445–446**: 126–135. doi:10.1016/j.scitotenv.2012.12.034

Hintelmann, H., and others. 2002. Reactivity and mobility of new and old mercury deposition in a boreal forest ecosystem during the first year of the METAALICUS study. Environ. Sci. Technol. **36**: 5034–5040. doi:10.1021/es025572t

Jiang, T., A. G. Bravo, U. Skyllberg, E. Björn, D. Wang, H. Yan, and N. W. Green. 2018. Influence of dissolved organic matter (DOM) characteristics on dissolved mercury (Hg) species composition in sediment porewater of lakes from southwest China. Water Res. **146**: 146–158. doi:10.1016/j.watres.2018.08.054

Jiskra, M., J. G. Wiederhold, U. Skyllberg, R.-M. Kronberg, I. Hajdas, and R. Kretzschmar. 2015. Mercury deposition and re-emission pathways in boreal forest soils investigated with Hg isotope signatures. Environ. Sci. Technol. **49**: 7188–7196. doi:10.1021/acs.est.5b00742

Johnson, K. B., T. A. Haines, J. S. Kahl, S. A. Norton, A. Amirbahman, and K. D. Sheehan. 2007. Controls on mercury and methylmercury deposition for two watersheds in Acadia National Park, Maine. Environ. Monit. Assess. **126**: 55–67. doi:10.1007/s10661-006-9331-5

Karimi, R., C. Y. Chen, P. C. Pickhardt, N. S. Fisher, and C. L. Folt. 2007. Stoichiometric controls of mercury dilution by growth. Proc. Natl. Acad. Sci. USA **104**: 7477–7482. doi:10.1073/pnas.0611261104

Kerimoglu, O., and K. Rinke. 2013. Stratification dynamics in a shallow reservoir under different hydro-meteorological scenarios and operational strategies: Nonwinter stratification dynamics. Water Resour. Res. **49**: 7518–7527. doi:10.1002/2013WR013520

Kirk, J. L., and others. 2011. Response to comment on climate change and mercury accumulation in Canadian high and subarctic lakes. Environ. Sci. Technol. **45**: 6705–6706. doi:10.1021/es202053c

Klaminder, J., R. Bindler, J. Rydberg, and I. Renberg. 2008. Is there a chronological record of atmospheric mercury and lead deposition preserved in the mor layer (O-horizon) of boreal forest soils? Geochim. Cosmochim. Acta **72**: 703–712. doi:10.1016/j.gca.2007.10.030

Kolka, R. K., E. A. Nater, D. F. Grigal, and E. S. Verry. 1999. Atmospheric inputs of mercury and organic carbon into a forested upland/bog watershed. Water Air Soil Pollut. **113**: 273–294. doi:10.1023/A:1005020326683

Laudon, H., J. Seibert, S. Köhler, and K. Bishop. 2004. Hydrological flow paths during snowmelt: Congruence between hydrometric measurements and oxygen 18 in meltwater, soil water, and runoff. Water Resour. Res. **40**: W031021–W031029. doi:10.1029/2003WR002455

Mason, R. P., J. R. Reinfelder, and F. M. M. Morel. 1995. Bioaccumulation of mercury and methylmercury. Water Air Soil Pollut. **80**: 915–921. doi:10.1007/BF01189744

Meyers, P. A., and R. Ishiwatari. 1993. Lacustrine organic geochemistry—an overview of indicators of organic matter sources and diagenesis in lake sediments. Org. Geochem. **20**: 867–900. doi:10.1016/0146-6380(93)90100-P

Moser, K. A., and others. 2019. Mountain lakes: Eyes on global environmental change. Glob. Planet. Change **178**: 77–95. doi:10.1016/j.gloplacha.2019.04.001

MSC-E. 2018. Data of HMs and POPs for the EMEP region. Meteorological Synthesizing Centre-East [WWW document]. [accessed 2018 July 10]. Available from http://en.msceast.org/

Navrátil, T., J. Shanley, J. Rohovec, M. Hojdová, V. Penizek, and J. Buchtová. 2014. Distribution and pools of mercury in Czech forest soils. Water Air Soil Pollut. **225**: 1829. doi:10.1007/s11270-013-1829-1

Navrátil, T., J. B. Shanley, J. Rohovec, F. Oulehle, M. Šimeček, J. Houška, and P. Cudlín. 2016. Soil mercury distribution in adjacent coniferous and deciduous stands highly impacted by acid rain in the Ore Mountains, Czech Republic. Appl. Geochem. **75**: 63–75. doi:10.1016/j.apgeochem.2016.10.005

Obrist, D., and others. 2011. Mercury distribution across 14 U.-S. forests. Part I: Spatial patterns of concentrations in biomass, litter, and soils. Environ. Sci. Technol. **45**: 3974–3981. doi:10.1021/es104384m

Obrist, D., D. W. Johnson, and R. L. Edmonds. 2012. Effects of vegetation type on mercury concentrations and pools in two adjacent coniferous and deciduous forests. J. Plant Nutr. Soil Sci. **175**: 68–77. doi:10.1002/jpln.201000415

Ouellet, J.-F., M. Lucotte, R. Teisserenc, S. Paquet, and R. Canuel. 2009. Lignin biomarker as tracers of mercury in lakes water column. Biogeochemistry **94**: 123–140. doi:10.1007/s10533-009-9314-z

Outridge, P. M., H. Sanei, G. A. Stern, P. B. Hamilton, and F. Goodarzi. 2007. Evidence for control of mercury accumulation rates in Canadian High Arctic lake sediments by variations of aquatic primary productivity. Environ. Sci. Technol. **41**: 5259–5265. doi:10.1021/es070408x

Outridge, P. M., G. A. Stern, P. B. Hamilton, and H. Sanei. 2019. Algal scavenging of mercury in preindustrial Arctic

lakes. Limnol. Oceanogr. **64**: 1558–1571. doi:10.1002/lno.11135

Pickhardt, P. C., C. L. Folt, C. Y. Chen, B. Klaue, and J. D. Blum. 2002. Algal blooms reduce the uptake of toxic methylmercury in freshwater food webs. Proc. Natl. Acad. Sci. USA **99**: 4419–4423. doi:10.1073/pnas.072531099

Pompeani, D. P., C. A. Cooke, M. B. Abbott, and P. E. Drevnick. 2018. Climate, fire, and vegetation mediate mercury delivery to midlatitude lakes over the holocene. Environ. Sci. Technol. **52**: 8157–8164. doi:10.1021/acs.est.8b01523

Rydberg, J., J. Karlsson, R. Nyman, I. Wanhatalo, K. Näthe, and R. Bindler. 2010. Importance of vegetation type for mercury sequestration in the northern Swedish mire, Rödmossamyran. Geochim. Cosmochim. Acta **74**: 7116–7126. doi:10.1016/j.gca.2010.09.026

Rydberg, J., and A. Martinez-Cortizas. 2014. Geochemical assessment of an annually laminated lake sediment record from northern Sweden: A multi-core, multi-element approach. J. Paleolimnol. **51**: 499–514. doi:10.1007/s10933-014-9770-x

Rydberg, J., M. Rösch, E. Heinz, and H. Biester. 2015. Influence of catchment vegetation on mercury accumulation in lake sediments from a long-term perspective. Sci. Total Environ. **538**: 896–904. doi:10.1016/j.scitotenv.2015.08.133

Sanei, H., P. M. Outridge, A. Dallimore, and P. B. Hamilton. 2012. Mercury–organic matter relationships in pre-pollution sediments of thermokarst lakes from the Mackenzie River Delta, Canada: The role of depositional environment. Biogeochemistry **107**: 149–164. doi:10.1007/s10533-010-9543-1

Schütze, M., G. Tserendorj, M. Pérez-Rodríguez, M. Rösch, and H. Biester. 2018. Prediction of holocene mercury accumulation trends by combining palynological and geochemical records of lake sediments (Black Forest, Germany). Geosciences **8**: 358. doi:10.3390/geosciences8100358

Schwesig, D., and E. Matzner. 2000. Pools and fluxes of mercury and methylmercury in two forested catchments in Germany. Sci. Total Environ. **260**: 213–223. doi:10.1016/s0048-9697(00)00565-9

Sheehan, K. D., I. J. Fernandez, J. S. Kahl, and A. Amirbahman. 2006. Litterfall mercury in two forested watersheds at Acadia National Park, Maine, USA. Water Air Soil Pollut. **170**: 249–265. doi:10.1007/s11270-006-3034-y

Siudek, P., M. Frankowski, and J. Siepak. 2016. Atmospheric particulate mercury at the urban and forest sites in central Poland. Environ. Sci. Pollut. Res. Int. **23**: 2341–2352. doi:10.1007/s11356-015-5476-5

Smolander, A., J. Loponen, K. Suominen, and V. Kitunen. 2005. Organic matter characteristics and C and N transformations in the humus layer under two tree species, *Betula pendula* and *Picea abies*. Soil Biol. Biochem. **37**: 1309–1318. doi:10.1016/j.soilbio.2004.12.002

Soerensen, A. L., A. T. Schartup, E. Gustafsson, B. G. Gustafsson, E. Undeman, and E. Björn. 2016. Eutrophication increases phytoplankton methylmercury concentrations in a coastal sea—a Baltic Sea case study. Environ. Sci. Technol. **50**: 11787–11796. doi:10.1021/acs.est.6b02717

St. Louis, V. L., and others. 2019. Atmospheric concentrations and wet/dry loadings of mercury at the remote experimental lakes area, northwestern Ontario, Canada. Environ. Sci. Technol. **53**: 8017–8026. doi:10.1021/acs.est.9b01338

Steinhoefel, G., J. Breuer, F. von Blanckenburg, I. Horn, and M. Sommer. 2017. The dynamics of Si cycling during weathering in two small catchments in the Black Forest (Germany) traced by Si isotopes. Chem. Geol. **466**: 389–402. doi:10.1016/j.chemgeo.2017.06.026

Teisserenc, R., M. Lucotte, and S. Houel. 2011. Terrestrial organic matter biomarkers as tracer of Hg sources in lake sediments. Biogeochemistry **103**: 235–244. doi:10.1007/s10533-010-9458-x

Thevenon, F., S. Guédron, M. Chiaradia, J.-L. Loizeau, and J. Poté. 2011. (Pre-) historic changes in natural and anthropogenic heavy metals deposition inferred from two contrasting Swiss Alpine lakes. Quat. Sci. Rev. **30**: 224–233.

Travnikov, O., and I. Ilyin. 2005. Regional model MSCE-HM of heavy metal transboundary air pollution in Europe. Technical report. Meteorological Synthesizing Centre-East (MSC-E). Russian Federation. https://scholar.google.com/scholar_lookup?title=Regional+Model+MSCE-HM+of+Heavy+Metal+Transboundary+Air+Pollution+in+Europe&author=Travnikov,+O.&author=Ilyin,+I.&publication_year=2005.

Tsz-Ki Tsui, M., and others. 2019. Controls of methylmercury bioaccumulation in forest floor food webs. Environ. Sci. Technol. **53**: 2434–2440. doi:10.1021/acs.est.8b06053

Wang, F., P. M. Outridge, X. Feng, B. Meng, L.-E. Heimbürger-Boavida, and R. P. Mason. 2019. How closely do mercury trends in fish and other aquatic wildlife track those in the atmosphere? – implications for evaluating the effectiveness of the Minamata Convention. Sci. Total Environ. **674**: 58–70. doi:10.1016/j.scitotenv.2019.04.101

Wiener, J. G., and others. 2006. Mercury in soils, lakes, and fish in voyageurs national park (Minnesota): Importance of atmospheric deposition and ecosystem factors. Environ. Sci. Technol. **40**: 6261–6268. doi:10.1021/es060822h

Witt, E. L., R. K. Kolka, E. A. Nater, and T. R. Wickman. 2009. Influence of the forest canopy on total and methyl mercury deposition in the boreal forest. Water Air Soil Pollut. **199**: 3–11. doi:10.1007/s11270-008-9854-1

Woerndle, G. E., M. Tsz-Ki Tsui, S. D. Sebestyen, J. D. Blum, X. Nie, and R. K. Kolka. 2018. New insights on ecosystem mercury cycling revealed by stable isotopes of mercury in water flowing from a headwater peatland catchment. Environ. Sci. Technol. **52**: 1854–1861. doi:10.1021/acs.est.7b04449

Wohlgemuth, L., S. Osterwalder, C. Joseph, A. Kahmen, G. Hoch, C. Alewell, and M. Jiskra. 2020. A bottom-up

quantification of foliar mercury uptake fluxes across Europe. Biogeosciences. doi:10.5194/bg-2020-289

Zaferani, S., M. Pérez-Rodríguez, and H. Biester. 2018. Diatom ooze—a large marine mercury sink. Science **361**: 797–800. doi:10.1126/science.aat2735

Zhang, Y., L. Jaeglé, L. Thompson, and D. G. Streets. 2014. Six centuries of changing oceanic mercury. Global Biogeochem. Cycles **28**: 1251–1261. doi:10.1002/2014GB004939

Acknowledgments

This research was supported by the German Science Foundation (DFG Research Grants to H. Biester: BI 734/15-1). We appreciate the essential help of A. Calean and P. Schmidt with sample preparation and laboratory analyses. Special thanks to M. Andrezejewsky and A. Alten for supporting the fieldwork. We thank D. McLagan, C. Baptista-Salazar, and A. Lucassen for their helpful comments and suggestions to improve the manuscript. Thanks to Biolab Umweltanalysen GmbH for the use of the scanning electron microscope. We are also thankful to the editor K. D. Hambright and the anonymous reviewers for their helpful comments. Open Access funding enabled and organized by Projek deal.

Conflict of Interest

None declared.

Submitted 08 May 2020
Revised 22 September 2020
Accepted 03 December 2020

Associate editor: Yong Liu